

# Supplementary Information

## Dysregulated GABA/glutamate neuron differentiation in autism spectrum disorders with macrocephaly

Jessica Mariani, Gianfilippo Coppola, Ping Zhang, Alexej Abyzov, Lauren Provini, Livia Tomasini, Mariangela Amenduni, Anna Szekely, Dean Palejev, Michael Wilson, Mark Gerstein, Elena Grigorenko, Katarzyna Chawarska, Kevin Pelphrey, James Howe, Flora M. Vaccarino

### Content

Table of Content.....	1
<b>Supplementary Results</b>	
Genomic Analyses .....	2
Characterization of cortical organoids from ASD families .....	2
<b>Extended Data Figures</b> .....	<b>4</b>
Extended Data Fig. 1   Family structure of the subjects and differentiation protocol .....	4
Extended Data Fig. 2   Characterization of iPSC lines.....	5
Extended Data Fig. 3   Expression of endogenous/exogenous reprogramming factors in iPSCs.....	6
Extended Data Fig. 4   Inherited copy number variants (CNVs) intersecting with genes in the SFARI dataset .....	8
Extended Data Fig. 5   ASD organoids neuronal differentiation potential .....	9
Extended Data Fig. 6   Transcriptome correlation between iPSC-derived organoids and postmortem human brain samples.....	10
Extended Data Fig. 7   Voltage-activated currents in iPSC-derived neurons.....	11
Extended Data Fig. 8   iPSC-derived neurons form functional synapses.....	12
Extended Data Fig. 9   Decreased cell cycle length and increased neuronal/synaptic differentiation in ASD proband.....	13
Extended Data Fig.10  Excitatory and inhibitory neuronal lineages arise in distinct areas of the organoids.....	14
Extended Data Fig.11 GABAergic transcription factors show enhanced expression in ASD-derived organoids.....	15
Extended Data Fig.12  Proliferation in proband- and control-derived organoids.....	16
Extended Data Fig.13  Not significant or transient changes in the proportion of excitatory progenitors after FOXP1-knockdown.....	18
<b>Supplementary References</b> .....	<b>20</b>
<b>Supplementary Tables</b> .....	<b>21-29</b>
Supplementary Table 1   Participant characteristics (external XLS file).	
Supplementary Table 2   Differentially expressed genes (external XLS file).	
Supplementary Table 3   Validation of RNAseq calls by qPCR.....	23
Supplementary Table 4   List of genes in the 24 modules inferred by WGCNA (external XLS file).	
Supplementary Table 5   Overlap between the DEGs and the WGCNA modules (external XLS file).	
Supplementary Table 6   Functional Enrichment analysis according to DAVID for the top differentially expressed modules (external XLS file).	
Supplementary Table 7   Enrichment analysis results according to the Canonical Pathways database in MSigDB v4.0 for the top differentially expressed modules (external XLS file).	
Supplementary Table 8  List of top 100 most connected genes (hubs) for the top differentially expressed modules (external XLS file).	
Supplementary Table 9   Primers for qPCR.....	29

## Supplementary Information

### Supplementary Results

#### Genomic analyses

Whole genome sequencing data was obtained for DNA extracted from fibroblast samples and from iPSC lines for members of all five families in this study. Data were analyzed with CNVnator<sup>1</sup> for copy number variations (CNVs) discovery and with a GATK-based pipeline for single nucleotide variation (SNV) discovery (see **Methods**). CNVnator discovers CNVs using a read depth approach. For three families with both parents participating in the study (03, 07, and 1123), we predicted *de novo* CNVs and SNVs. Of the putative *de novo* CNVs, only one 4.8 kbp deletion in chr14:39987476-39992327 of the 1123 proband could be validated by qPCR. For this event, qPCR validation showed roughly 30% copy-number decrease in the proband relative to either of the parent. True *de novo* heterozygous germline deletion should result in 50% decrease for diploid chromosomes. Thus, the observed copy number decrease may suggest that the deletion is a somatic mosaic variant, i.e., not all cells in proband carry the deletion. This deletion did not overlap any known genes. Hence, we found none of the *de novo* CNVs intersected a gene causing syndromic ASD. Proband 07-03 carries a previously uncharacterized deletion involving exon 2 in the PTEN gene, which was also found in his unaffected father (**Extended data Fig. 4**). Proband 03-03 carries a small intronic deletion in CNTNAP2 gene. The deletion is heterozygous in parents, homozygous in the proband, and common in the human population (**Extended data Fig. 4**).

On average each proband had ~112,000 rare SNVs not previously detected by the 1000 Genomes Project. This is also likely to include most of *de novo* SNVs. By intersecting rare SNVs in probands with lists of genes whose disruption has been previously linked to ASD<sup>2</sup> as well as the SFARI syndromic genes dataset (<https://gene.sfari.org/autdb/Welcome.do>), we found no rare SNVs that cause a known deleterious loss of function of an ASD gene.

#### Characterization of cortical organoids from ASD families

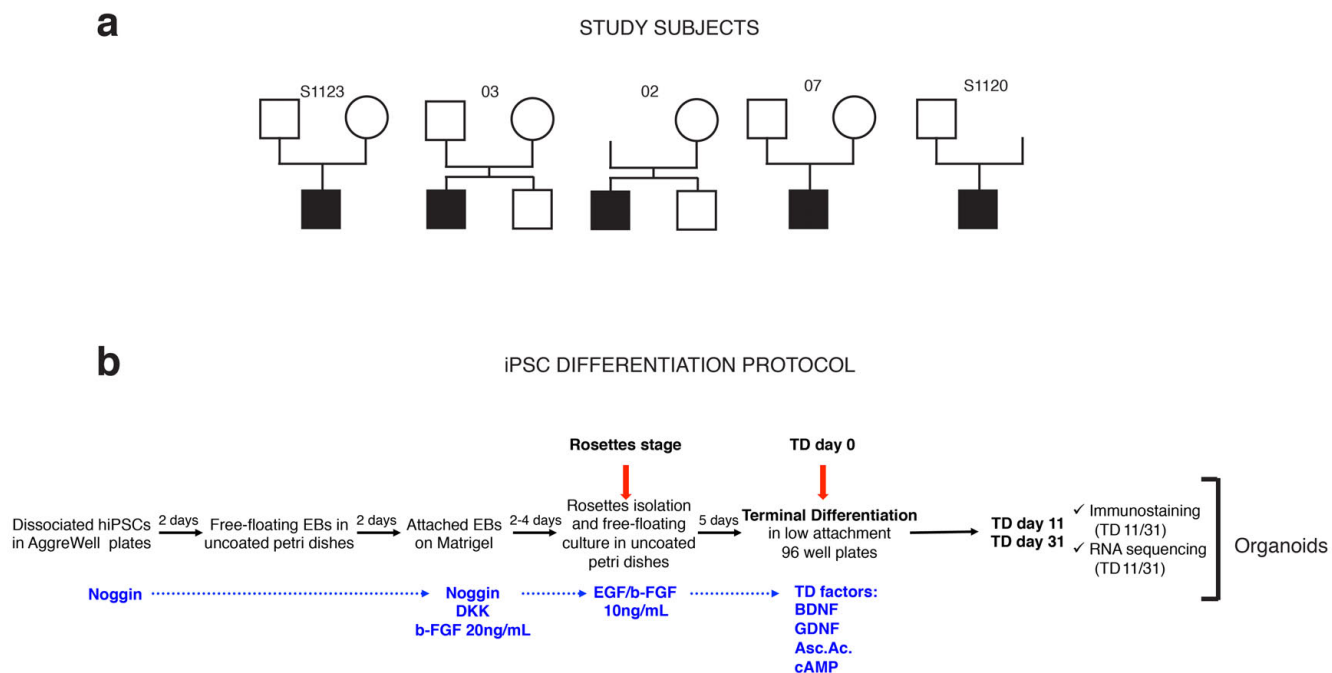
The iPSC lines from families 1123 and 03 have been previously characterized<sup>10</sup>, and the characterization for families 07 and 1120 is shown in **Extended Data Fig. 2 and 3**. The number of iPSC clones for each family member used in this study varied from two to three. We differentiated these lines into telencephalic neurons using a modification of our free-floating tridimensional (3D) culture method<sup>11</sup>. Briefly, floating aggregates composed of manually isolated neural rosettes, which are early neural progenitors, were kept in suspension for one week in the presence of growth factors and then for four to five weeks under conditions favoring terminal differentiation (see **Methods** and schematic outline in **Extended Data Fig. 1b**). After 11 days of terminal differentiation (TD11), the free-floating neural cell aggregates (referred to as organoids) were composed of polarized, proliferating radial glial cells expressing BLBP, NESTIN, PAX6, BRN2, SOX1/2, and Ki67. The radial glial cells underwent mitoses on the apical (luminal) side, whereas neuronal precursor cells expressing DCX and TUBB3 (and more mature NeuN<sup>+</sup> neurons at TD31) accumulated on the basal side of the layer of radial glial cells (**Fig. 2a,b; Extended Data Fig. 5a,b**). This is similar to the organization of our previously published preparation<sup>3</sup>. Both ASD-derived and unaffected family member-derived iPSCs had an equivalent potential to generate neuronal cells (**Extended Data Fig. 5**). We next analyzed global gene expression by RNAseq. Comparing the transcriptome of organoids at each of three time points (rosette stage, TD11, and TD31, two to three iPSC clones per individual, total 45 samples) with the transcriptome of the BrainSpan dataset<sup>4</sup>, we found that this preparation best reflected the transcriptome of the human cerebral cortex during the first trimester of gestation (9 weeks post conception) (**Extended Data Fig. 6**).

To compare the electrical excitability of iPSC-derived neurons from probands with those from familial controls, we made whole-cell patch-clamp recordings from neurons in dissociated cultures or at the edge of organoids. All neurons examined (n=99) expressed voltage-activated sodium and potassium currents that were of similar amplitude in control and proband neurons from two different families

**(Extended Data Fig. 7).** In recordings from cells in the organoids, the voltage-activated currents supported action potential firing in 18/18 control neurons and 12/14 proband neurons, with thresholds of  $-42.5 \pm 0.8$  mV and  $-37.9 \pm 2.1$  mV (controls, probands;  $P = 0.06$ ) and action potential overshoots of 30 to 65 mV. Most neurons fired only a single action potential, but some fired multiple spikes (**Extended Data Fig. 7**). In addition to these signatures of electrical excitability, we also recorded spontaneous synaptic currents in some neurons (**Extended Data Fig. 8**). In total, the electrophysiological data support the conclusion that the cells studied here display the phenotype of central neurons.

## Extended Data Figures

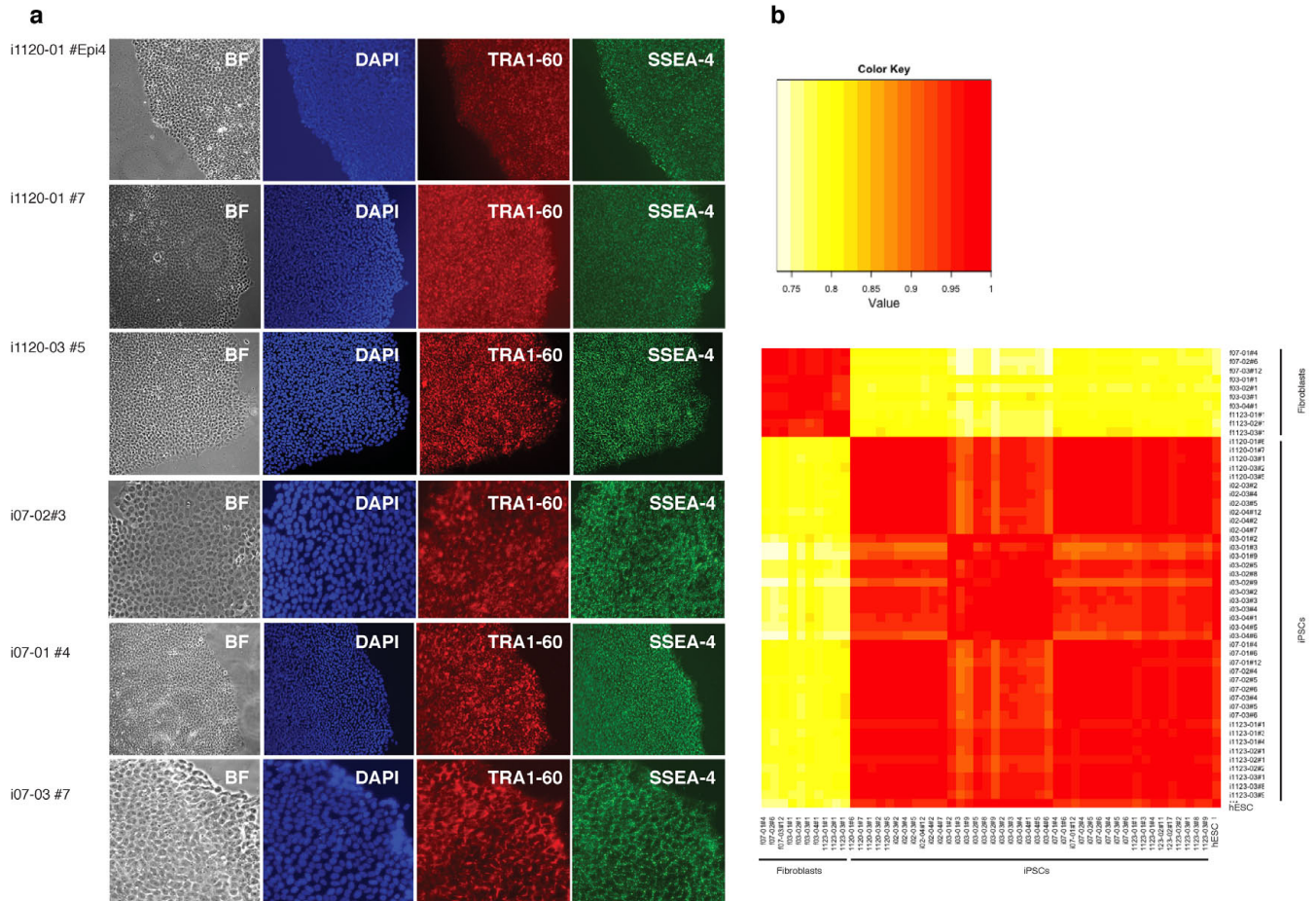
### Extended Data Figure 1



**Extended Data Figure 1. Schematic view of the family structure of the subjects and of the differentiation protocol used in this study.** **a**, Square symbols indicate males subjects, circles indicate females, and shaded symbols indicate individuals affected by ASD. **b**, For the neuronal differentiation we modified our previously published 3D organoid culture<sup>3</sup> by combining it with a monolayer protocol<sup>5</sup>. Our previous protocol showed that neural progenitors kept in a 3D conformation were able to differentiate and recapitulate early aspects of forebrain development<sup>3</sup>. To improve its efficiency we added a neural rosette step<sup>5</sup> to enrich for neural progenitor cells (see Methods for details). The neural rosettes were cultured in suspension for five days in EGF and FGF and kept as free-floating undissociated organoids during terminal differentiation (TD). Organoids were analyzed by RNA sequencing and immunocytochemistry at different time points during the neuronal differentiation (TD11 and TD31) (see Methods for details), except when evaluating cell cycle/proliferation of the neuronal progenitors at TD11, for which the neural rosettes were dissociated into single cells and cultured in adhesion as monolayers.

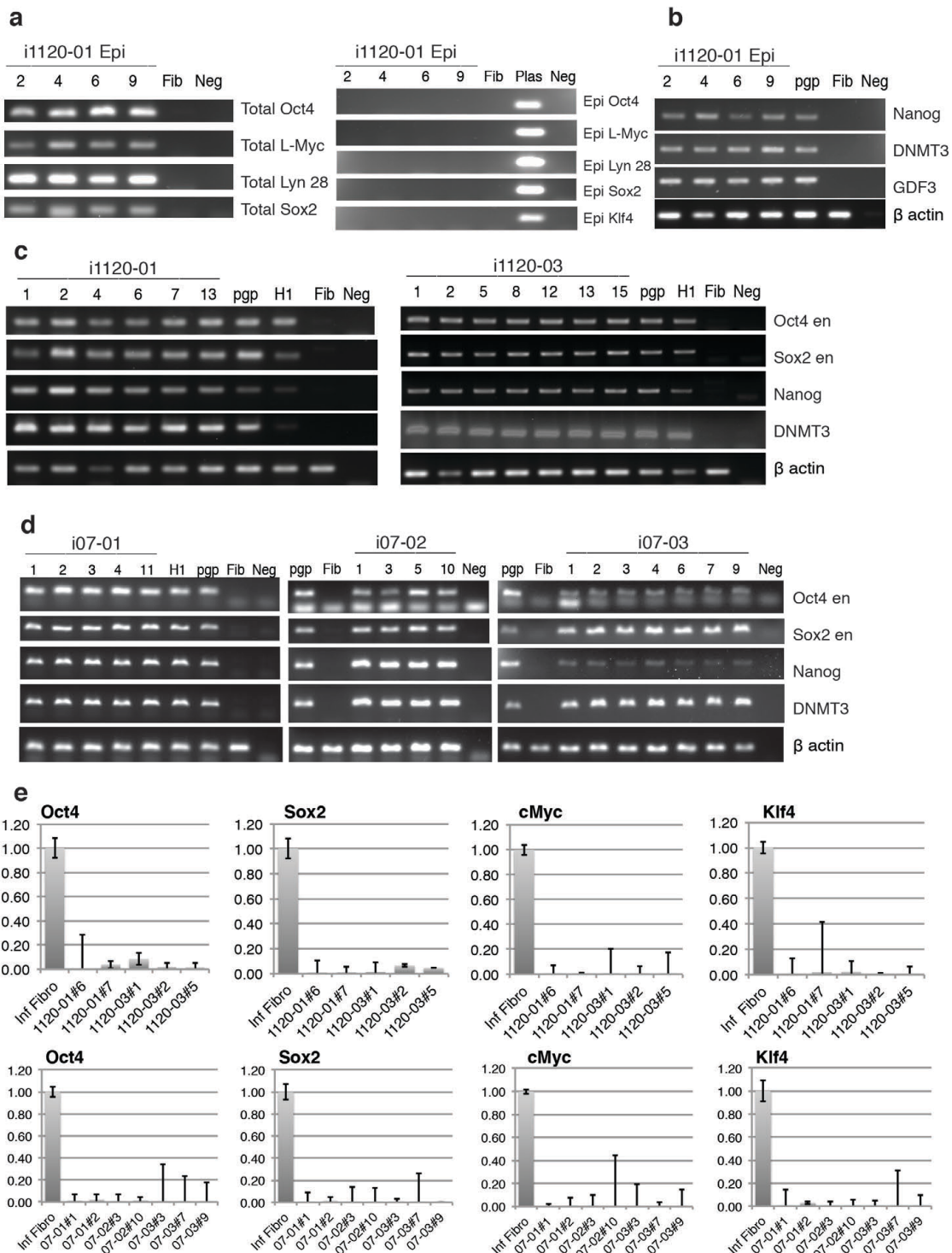


## Extended Data Figure 2



**Extended Data Figure 2. Characterization of iPSC lines.** **a**, Bright field (BF) morphology and expression of endogenous pluripotency markers by immunofluorescence. **b**, Hierarchical clustering of RNAseq [ $\log_2(\text{RPKM}+1)$ ] data from iPSCs lines and fibroblasts in our dataset, as well as hESCs (H1 line). Red squares show clustering of iPSC with each other and H1 but not with fibroblasts.

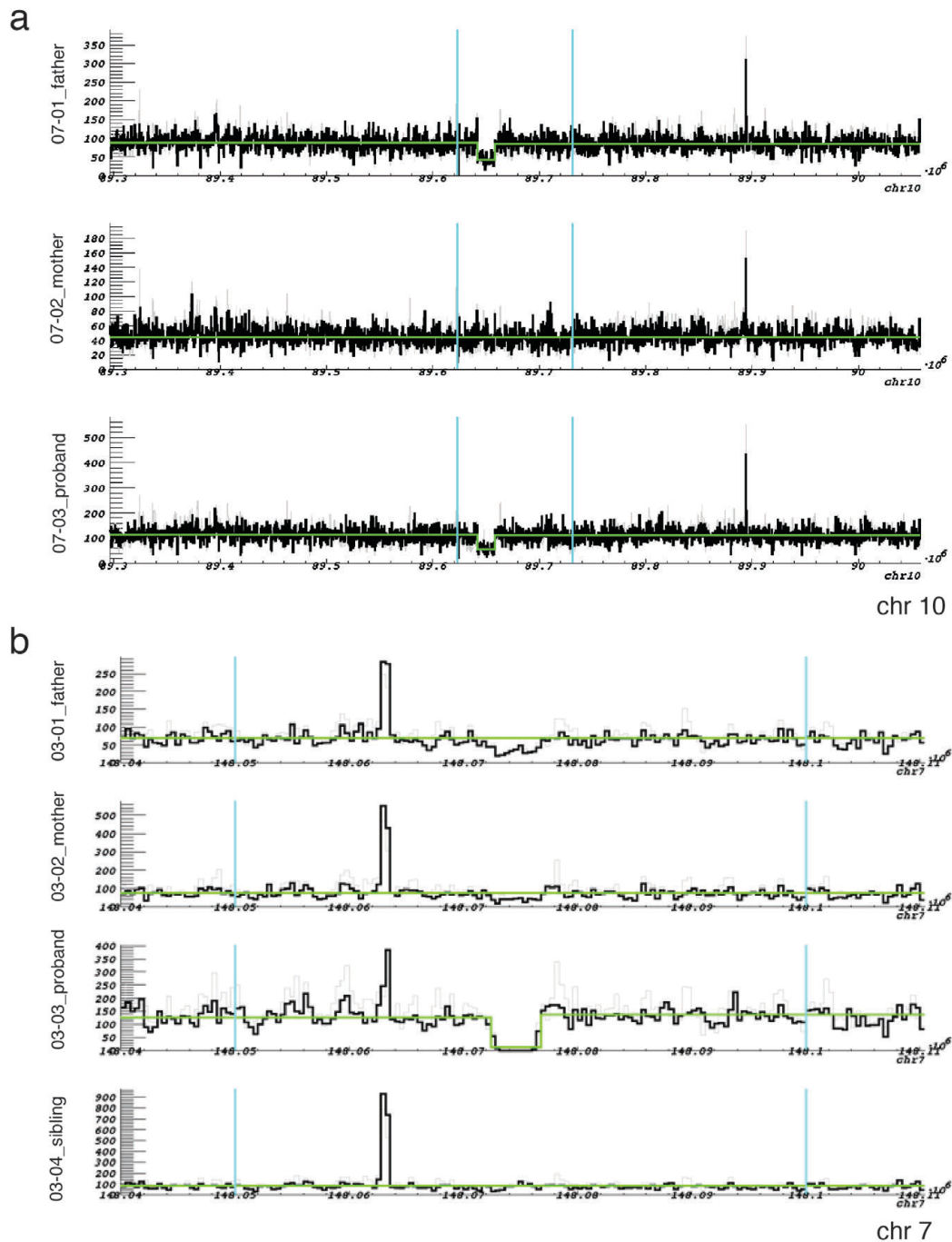
### Extended Data Figure 3



**Extended Data Figure 3. Expression of endogenous/exogenous reprogramming factors in iPSCs.** **a**, RT-PCR analyses for endogenous and exogenous (total) reprogramming genes and exogenous episomal genes (Epi) in iPSC clones from family 1120 generated by a viral-free episomal reprogramming method<sup>6</sup> (see methods). PGP-1-1 (pgp) is a control retrovirus-derived iPSC line used as a comparison. Fibroblast (Fib) and PCR Negative control (Neg) were used as negative controls; Plas indicates plasmid positive control. **b**, Expression of pluripotent cell

markers in the same episomal reprogrammed lines. **c,d**, Expression of pluripotent cell markers by RT-PCR analysis in iPSC clones for families 1120 (**c**) and 07 (**d**) generated by the standard retrovirus approach. OCT4 en and SOX2 en indicate expression of the endogenous reprogramming genes. The iPSC line PGP-1-1 (pgp) and hES line H1 were used as positive controls. Fibroblast (Fib) and PCR Negative control (Neg) were used as negative controls. **e**, Quantitative real time PCR assay for expression of the exogenous reprogramming genes OCT4, SOX2, c-MYC and KLF4 in retroviral-derived iPSC clones. Expression levels were calculated as average expression and normalized to the housekeeping gene GAPDH ( $2^{-ddCT_{mean}}$ ). Parental fibroblasts four days after viral infection were used as positive controls.

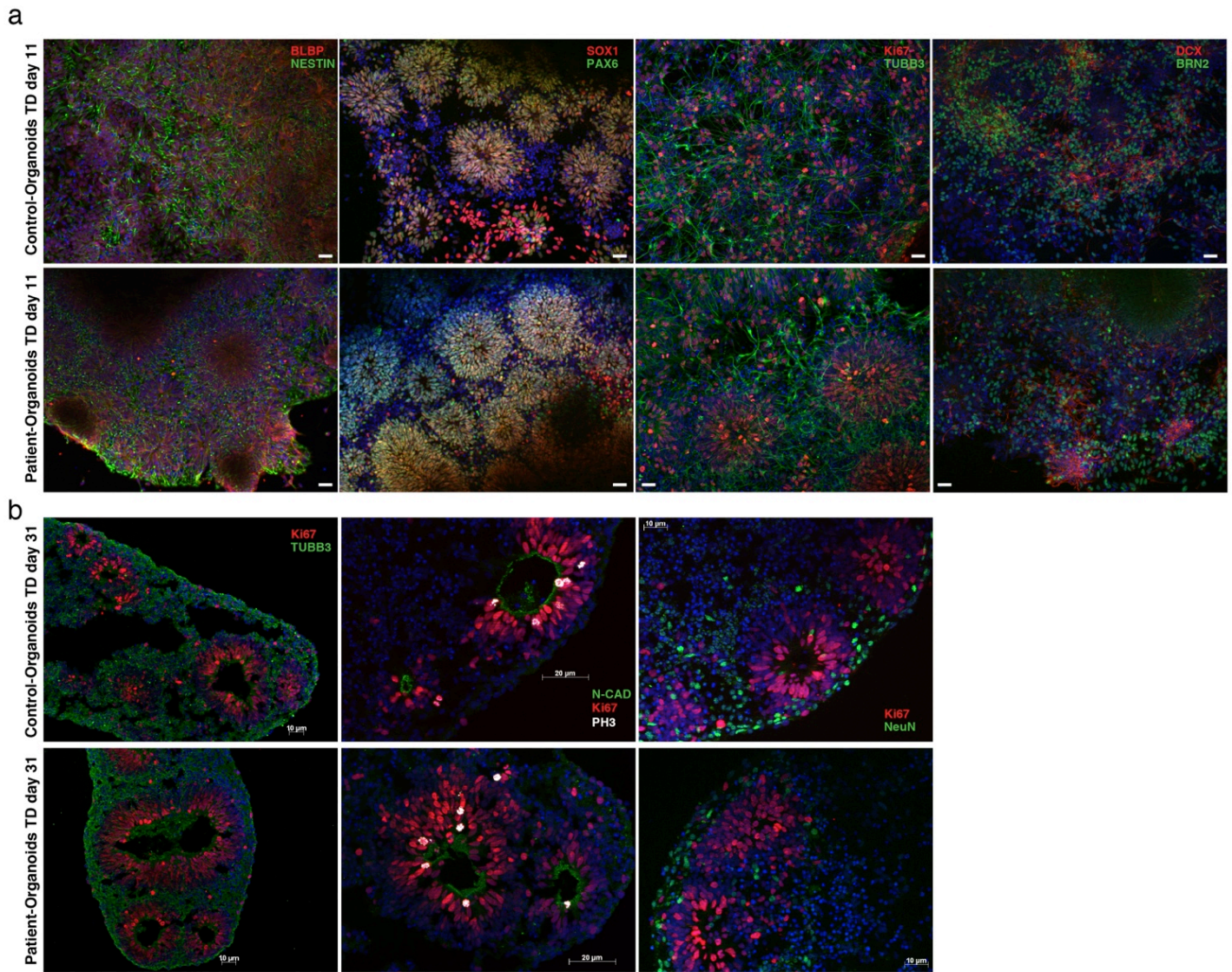
Extended Data Figure 4



**Extended Data Figure 4. Inherited copy number variants (CNVs) intersecting with genes in the SFARI dataset. a,b,** read depth tracks from whole genome sequencing data obtained in fibroblasts. **(a)** Heterozygous deletion (chr10:89,641,498-89,658,394) in proband of family 07 (07-03) involving exon 2 of the PTEN gene (chr10:89,623,195-89,728,532, delimited by cyan lines) inherited from the father. **(b)** Homozygous intronic deletion (chr7:148,072,760-148,076,444) involving the CNTNAP2 gene (chr7:145,813,453-148,118,088, delimited by cyan lines) in probands of family 03 (03-03). Parents are heterozygous for the deletion.

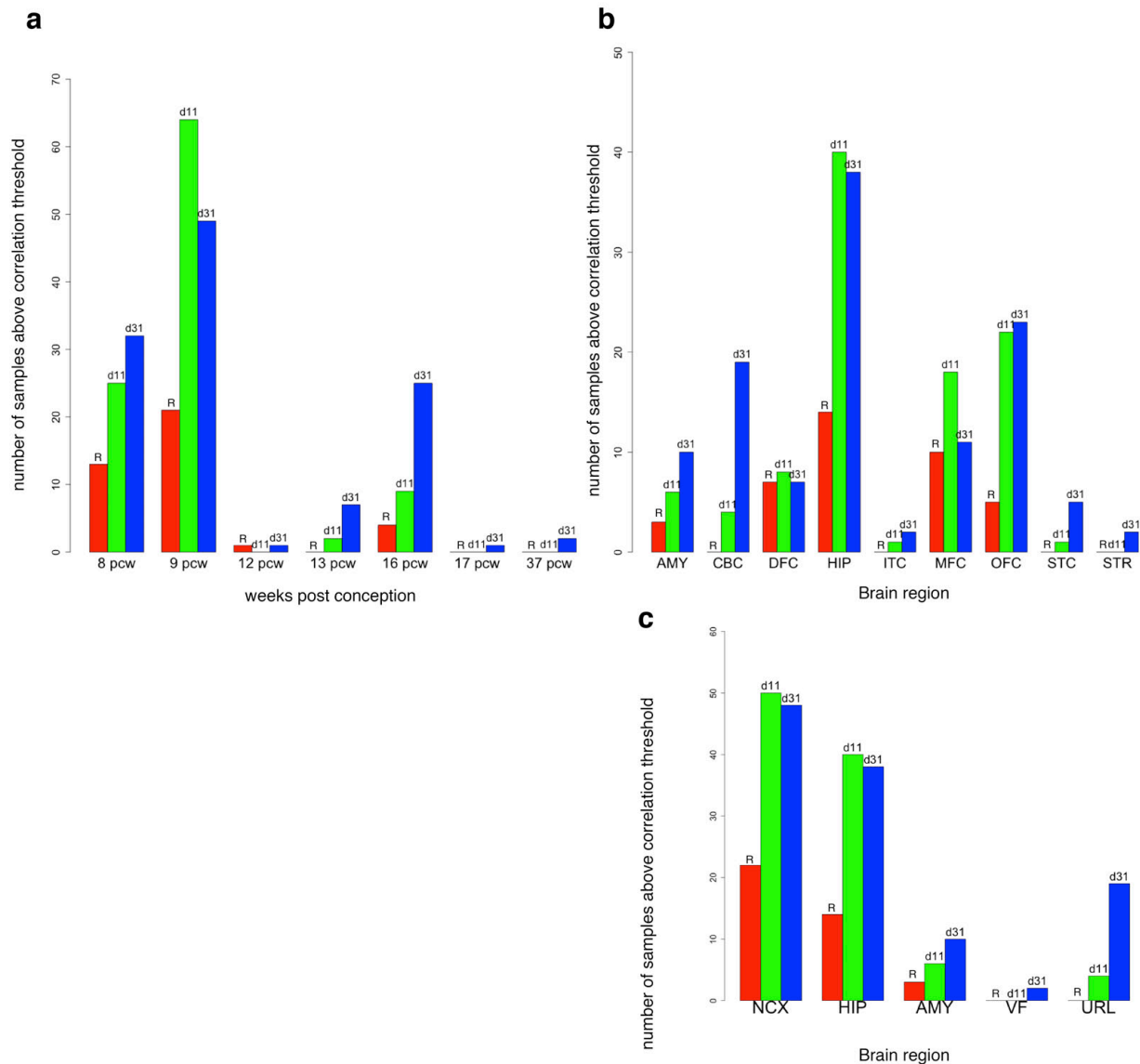


## Extended Data Figure 5



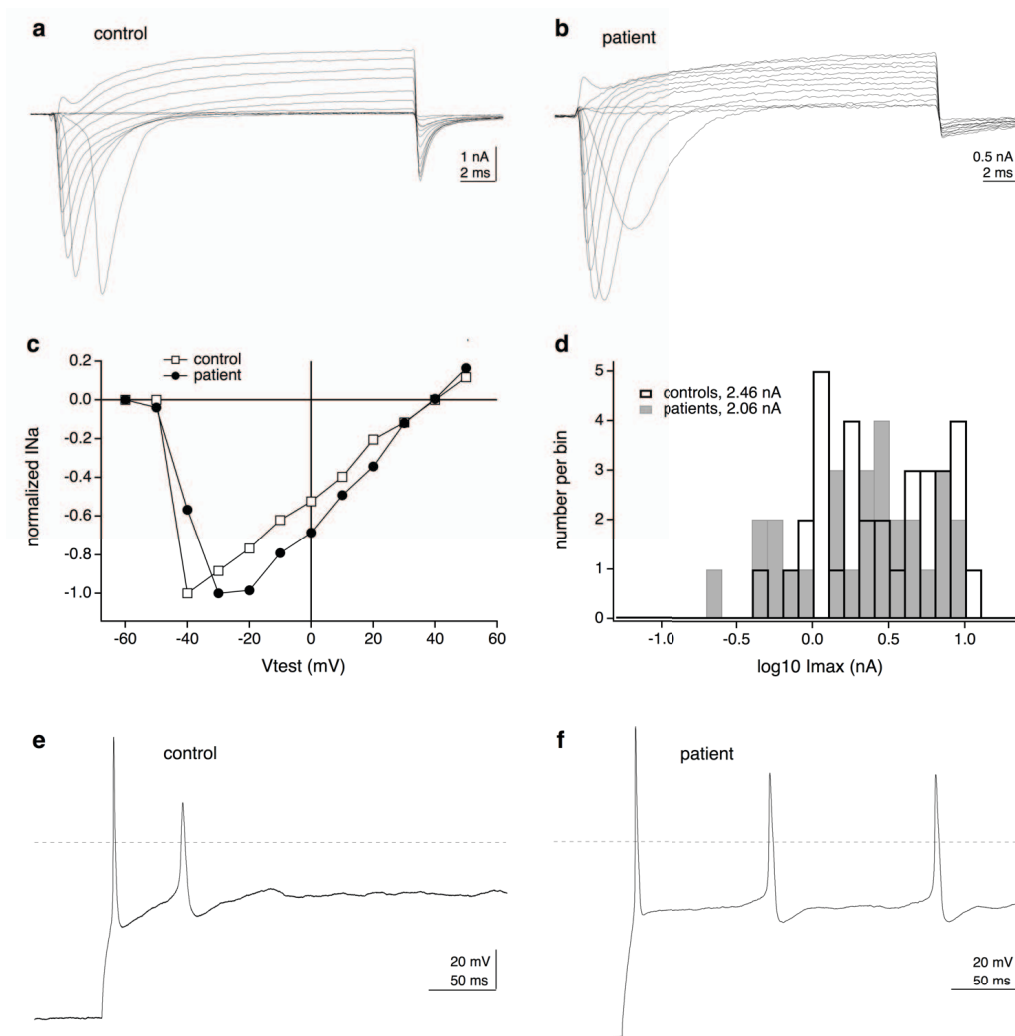
**Extended Data Figure 5. ASD organoids neuronal differentiation potential.** Representative images of control-derived and ASD-derived organoids at TD11 (**a**) and TD31 (**b**). Both control-derived and ASD-derived organoids express markers for proliferating neural progenitors (BLBP, NESTIN, SOX1, PAX6, BRN2, Ki67, pH3), and the neuronal markers TUBB3, DCX and NeuN. The organoids have apico-basal polarity with *N-CADHERIN*<sup>+</sup> apical end feet of radial glial cells and pH3<sup>+</sup> cells undergoing mitosis at the apical side of the neuroepithelium. Scale bars, 10 µm (**a**), 10-20 µm (as indicated in **b**).

## Extended Data Figure 6



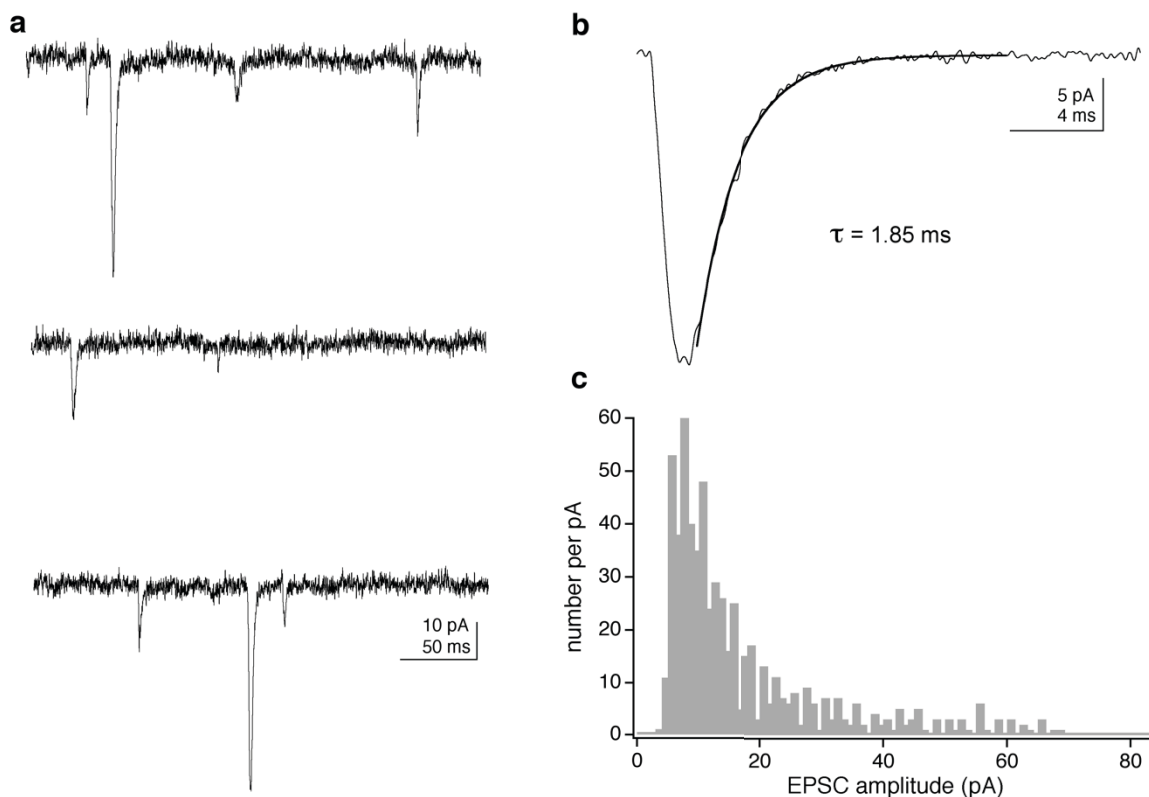
**Extended Data Figure 6. Transcriptome correlation between iPSC-derived organoids and postmortem human brain samples.** Correspondence of iPSC-derived neuronal organoids at the rosette (R) and terminal differentiation day 11 and 31 (d11 and d31) (n= 45 samples, for details see Supplementary Table 1) and postmortem human brain samples from the BRAINSPAN project. Each iPSC-derived neuronal sample was classified as corresponding to a particular brain sample by transcriptome correlation, i.e., if its correlation coefficient was within the 95% confidence interval of the maximum correlation coefficient. Average maximum correlation value is 0.86. **a**, X-axis is the postconceptional age in weeks of the BRAINSPAN postmortem brain samples. Y-axis is the number of times each iPSC-derived neuron sample was classified according to a certain age (shown on x-axis). **b**, X-axis shows BRAINSPAN brain regions: AMY, amygdala; CBC, cerebellar cortex; DFC, dorsolateral frontal cortex; HIP, hippocampus; ITC, inferolateral temporal cortex; MFC, anterior (rostral) cingulate (medial prefrontal) cortex; OFC, orbital frontal cortex; STC, posterior (caudal) superior temporal cortex (area 22c); STR, striatum. **c**, X-axis shows BRAINSPAN agglomerated brain regions: NCX, neo-cortex; HIP, hippocampus; AMY, amygdala; VF, ventral forebrain; URL, upper rhombic lip. Y-axis is the number of times each iPSC-derived neuron sample was classified according to a BRAINSPAN sample. As seen, the transcriptome of iPSC-derived organoids at any of the analyzed days of differentiation is most similar to that of the human dorsal telencephalon (cerebral cortex and hippocampus) during the first trimester of gestation (postconceptional weeks 8-16).

## Extended Data Figure 7



**Extended Data Figure 7. Voltage-activated currents in iPSC-derived neurons.** **a, b**, Currents evoked in neurons from a control (**a**) and a patient (**b**) by 20-ms test depolarizations from -60 mV to +50 mV (in 10 mV steps). The pre-pulse potential was -120 mV and the currents were leak-subtracted. Both rapidly activating sodium currents and more slowly activating outward currents are present. Similar currents were seen in all neurons examined in dissociated cultures (n=38) or organoids (n=61). The inward and outward currents were blocked by 1  $\mu$ M tetrotoxin (n=3) and 10 mM tetraethylammonium (n=4), respectively. The voltage dependence and kinetics of activation and inactivation of the inward currents are typical of sodium currents in central neurons. **c**, Current-voltage data for the fast sodium currents in panels (**a**) and (**b**). The inward currents reverse direction near +40 mV (results normalized to the maximum inward current recorded from each neuron). The mean reversal potential for similar currents was  $53.5 \pm 3.8$  mV for control neurons (n=12) and  $58.7 \pm 7.1$  mV for patient neurons (n=8). **d**, Histogram of the amplitude of maximum inward currents recorded from neurons along the edge of organoids (33 control and 28 patient neurons). The distribution of current sizes was log-normal (see Methods) and the control and patient data gave mean peak inward currents of 2.46 nA (2.37-3.22 nA) and 2.09 nA (1.72-2.54 nA), respectively (means and ranges are the anti-logs of mean  $\pm$  s.e.m. values from the log-transformed data). The size of the currents did not change significantly from 32 to 72 days in vitro. **e, f**, Action potentials elicited by depolarizing current injections in iPSC-derived neurons from a patient (**f**) and the corresponding parental control (**e**). The dashed lines indicate a membrane potential of 0 mV.

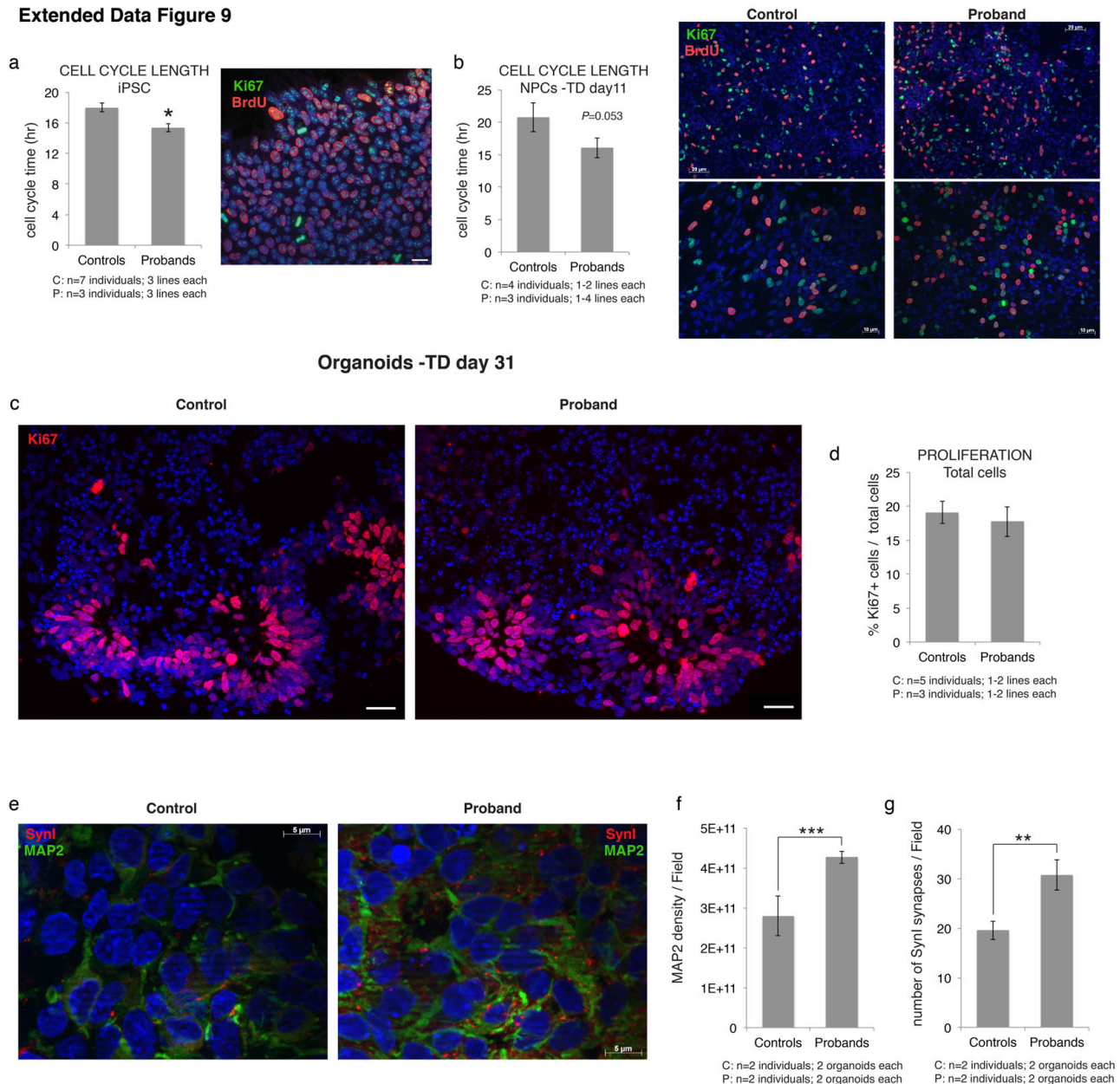
## Extended Data Figure 8



**Extended Data Figure 8. iPSC-derived neurons form functional synapses.** **a**, Examples of spontaneous excitatory postsynaptic currents (EPSCs) recorded at a holding potential of -70 mV in a neuron from a parental control that was maintained in vitro for 52 days. **b**, average EPSC obtained from 30 spontaneous events. The decay of the current was fitted with a single exponential that gave a time constant of 1.85 ms. **c**, Histogram of the amplitude of spontaneous inward EPSCs recorded from the same neuron (604 events). The overall frequency of events detected in this neuron was 0.81 per second. Similar results were obtained from two other control neurons. The fast rise (0.5-0.7 ms) and decay (1.8-2.4 ms) of these currents and their reversal near 0 mV strongly suggests that they were AMPA-receptor EPSCs. In two patient-derived neurons and one control neuron we saw occasional synaptic currents that were larger (40 to 325 pA, at -70 mV) and which decayed with time constants of 7 to 10 ms. The small number of these events did not allow us to characterize them further.



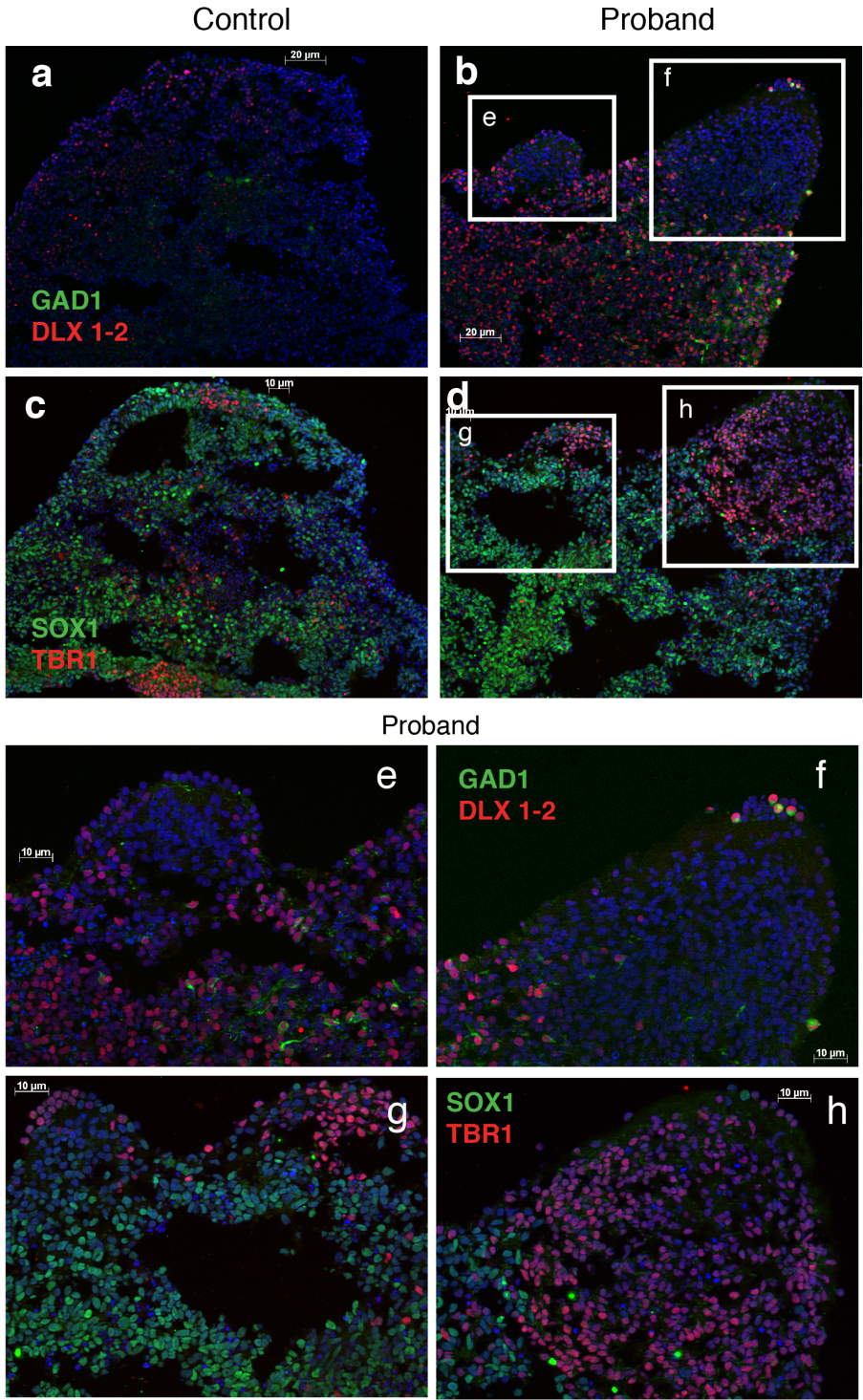
## Extended Data Figure 9



### Extended Data Figure 9. Decreased cell cycle length and increased neuronal/synaptic differentiation in ASD probands.

Double immunostaining for BrdU (red) and Ki67 (green) of undifferentiated iPSCs (a) and early neuronal progenitors (b). Cell cycle time was determined by the formula  $T_c = T_s / (\% \text{BrdU} / \text{Ki67})$ , where  $T_c$  = cell cycle time and  $T_s$  = S phase time. \*  $P < 0.05$ , ANOVA with family as covariant. c, d, Representative images (c) and stereological quantification (d) of the proportion of proliferating Ki67<sup>+</sup> neuronal progenitor cells in both control and ASD-derived organoids at TD31. c-g, Increased neuronal maturation and synaptic formation in ASD-derived neurons (TD 31). Representative images of controls and probands organoids at TD 31 labeled with MAP2 and Syn1 (e) and relative quantification of MAP2 density (f) and Syn1 number of puncta (g). The data in (f-g) are presented as means  $\pm$  s.e.m; \*\*  $P < 0.01$ , \*\*\*  $P < 0.001$ ; t test analysis. Scale bars, 10  $\mu\text{m}$  (a), 10-20  $\mu\text{m}$  (b, as indicated), 10  $\mu\text{m}$  (c), 5  $\mu\text{m}$  (e).

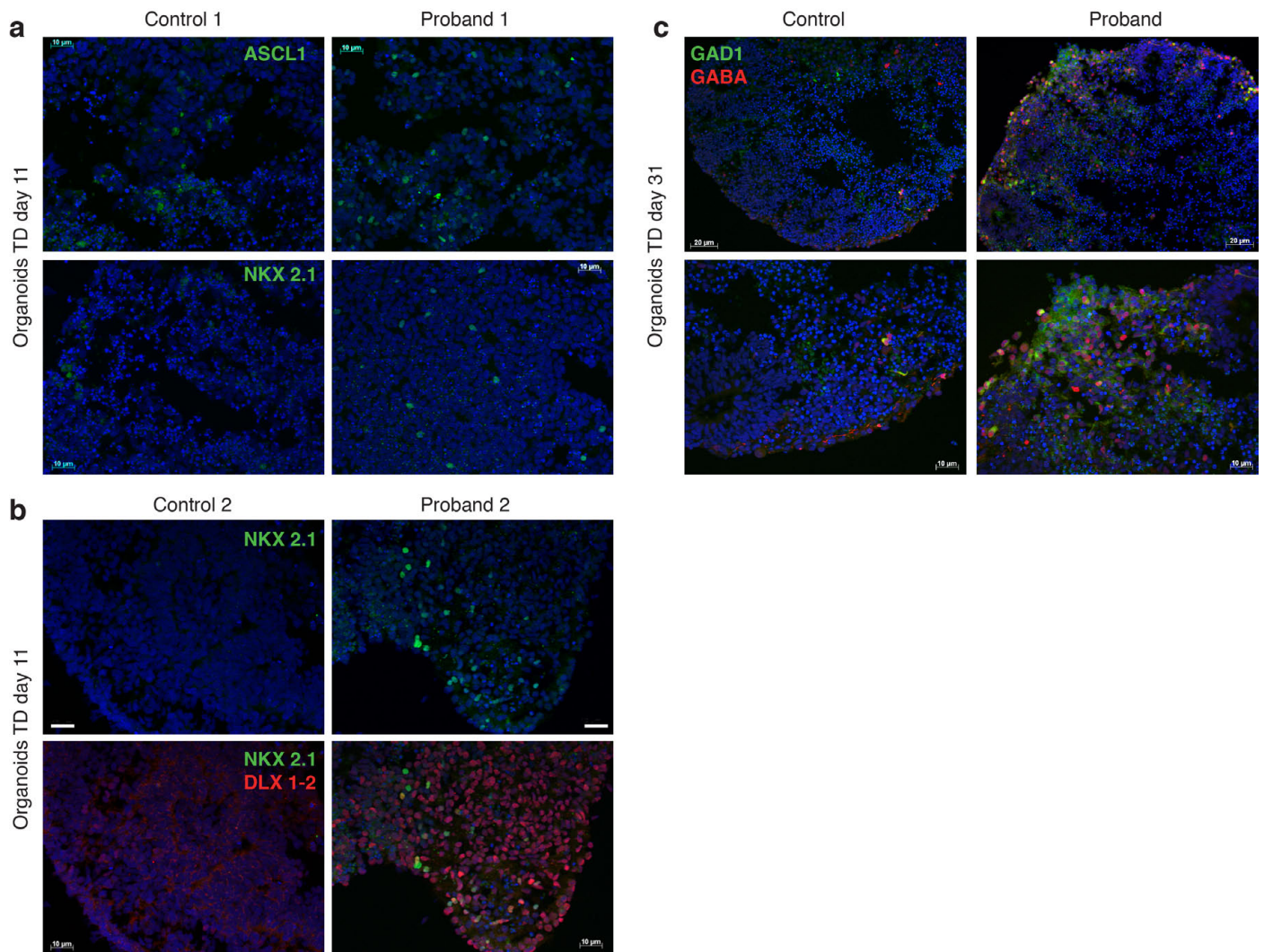
**Extended Data Figure 10**



**Extended Data Figure 10. Excitatory and inhibitory neuronal lineages arise in distinct areas of the organoids.** GABAergic progenitors (DLX1-2<sup>+</sup>) and mature interneurons (GAD1<sup>+</sup>) in control (a,c) and probands (b,d,e-h) at TD11 arise in restricted areas of the organoid devoid of excitatory neuronal progenitors expressing TBR1 (c,d) and Pax6/Tbr2 (not shown). Lower panels show high magnifications of areas in boxes e,f,g,h. Scale bars, 10-20 μm as indicated.



## Extended Data Figure 11

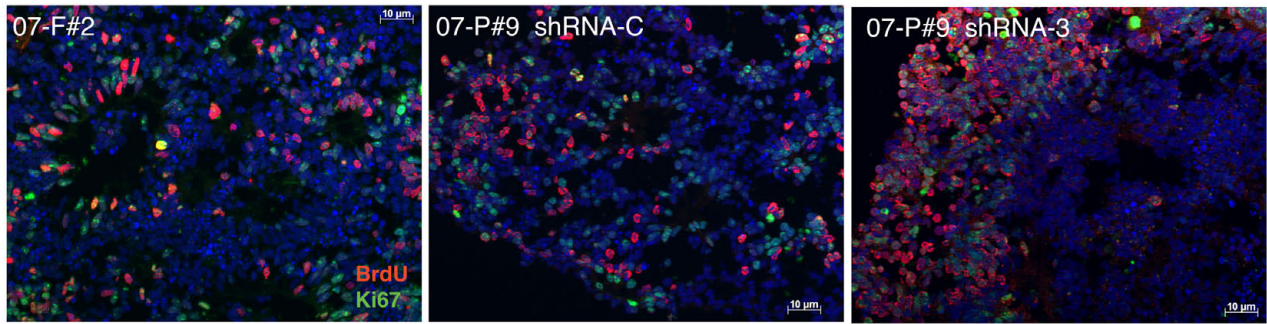


**Extended Data Figure 11. GABAergic transcription factors MASH1 and NKX2.1 and GABA show enhanced expression in ASD-derived organoids.** **a**, Representative images of control-derived and proband-derived organoids at TD11 labeled with antibodies against ASCL1/MASH1 and NKX2.1. **b**, Immunostaining for DLX1-2 and NKX2.1 of control-derived and proband-derived organoids at TD11. **c**, Double-immunostaining of control-derived and proband-derived organoids at TD31 labeled with antibodies against GAD1 and GABA. Scale bars, 10  $\mu\text{m}$  (**a**, **b**), 10-20  $\mu\text{m}$  (**c**, as indicated).

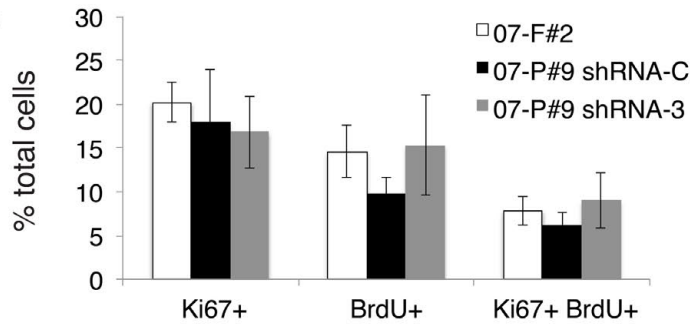
Extended Data Figure 12

**a**

Organoids -TD day 11

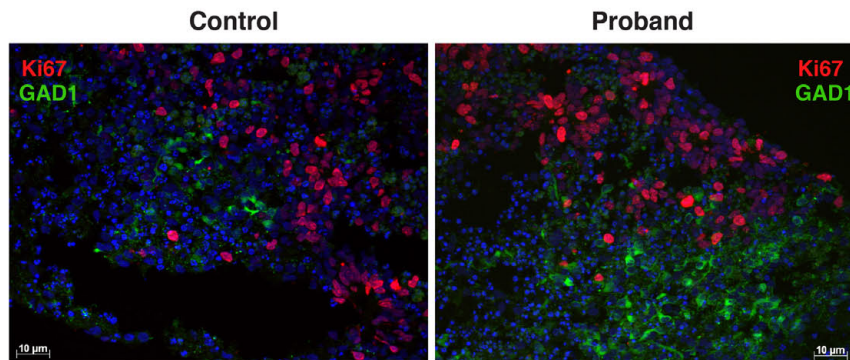


**b**

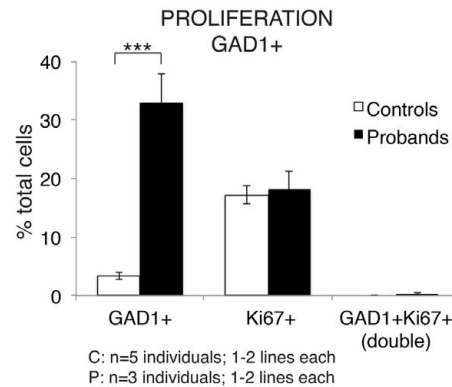


Organoids -TD day 31

**c**



**d**

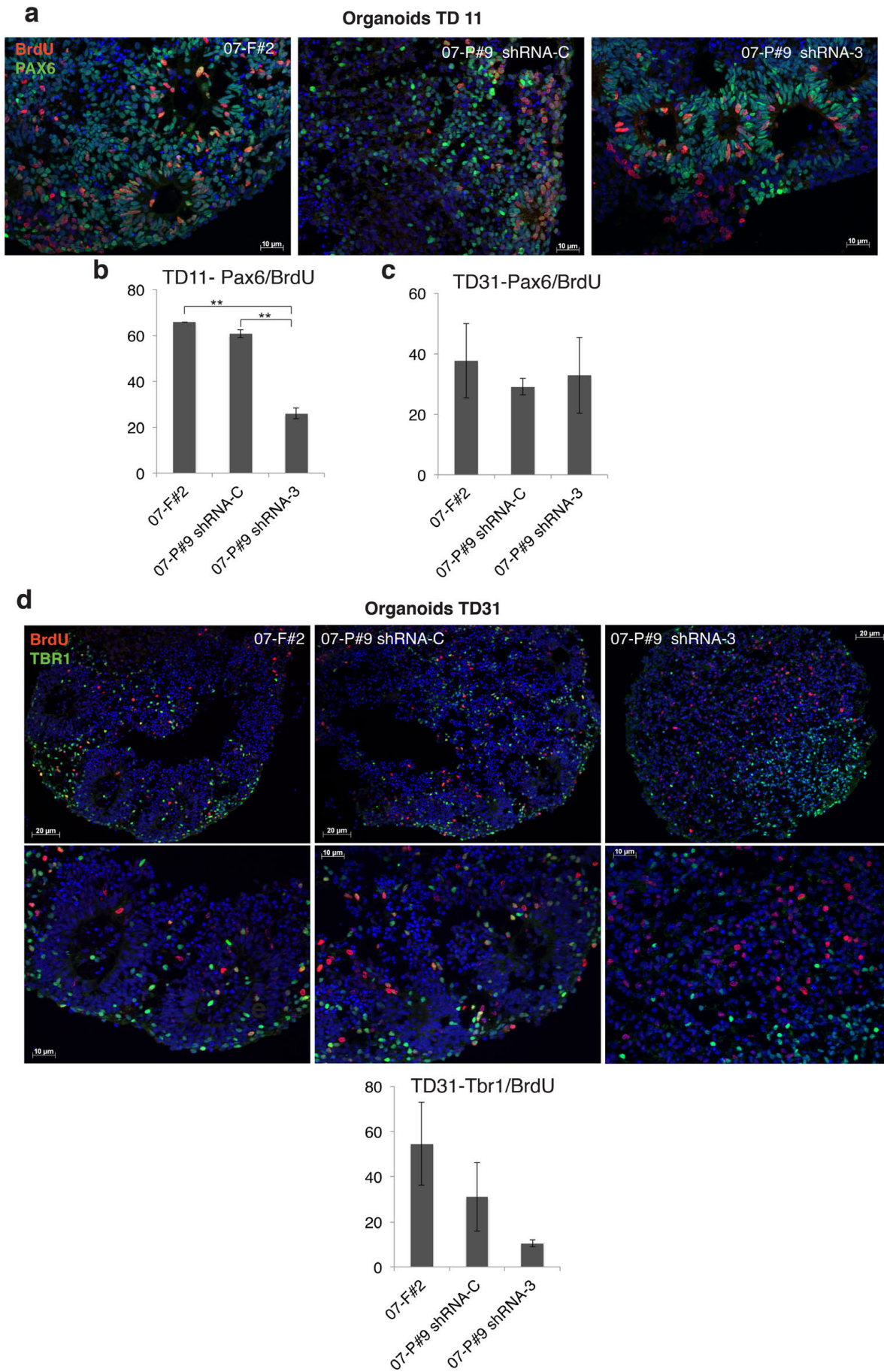


**Extended Data Figure 12. a, b, Proliferation in proband- and control-derived organoids.** Representative images and relative stereological quantification of BrdU<sup>+</sup> and Ki67<sup>+</sup> cells in TD11 organoids derived from 07-F#2, 07-P#9 shRNA-C, and 07-P#9 shRNA-3. Error bars are s.e.m. Scale bars, 10 μm. **c, d, Representative images of Ki67 and GAD1 double immunostaining and stereological**

quantification in organoids at TD31 in the indicated lines. Note that total proliferation as assessed by % Ki67<sup>+</sup> cells is not changed at this time point and that there is no aberrant proliferation of GABAergic mature interneurons at TD31. Error bars are s.e.m. \*\*\*  $P < 0.001$ , t test analysis. Scale bars, 10  $\mu\text{m}$ .



Extended Data Figure 13



**Extended Data Figure 13. Not significant or transient changes in the proportion of excitatory progenitors after FOXG1-knockdown.** **a-c**, Representative images (**a**) and stereological quantification (**b, c**) of PAX6<sup>+</sup>/BrdU<sup>+</sup> double positive excitatory progenitor cells over total BrdU<sup>+</sup> cells in TD11 and TD31 organoids with or without RNAi-mediated FOXG1 knockdown. **d, e**, Representative images (**d**) and stereological quantification (**e**) of TBR1<sup>+</sup>/BrdU<sup>+</sup> double positive excitatory neurons over total BrdU<sup>+</sup> neurons with or without RNAi-mediated FOXG1 knockdown. In all cases BrdU incorporation was at TD11 and analyses at TD11 or TD31. Error bars are s.e.m. \*\*  $P < 0.01$ , t test analysis. Scale bars, 10  $\mu\text{m}$  (**a**), 10-20 $\mu\text{m}$  (**d**).

## Supplementary References

- 1 Abyzov, A., Urban, A. E., Snyder, M. & Gerstein, M. CNVnator: An approach to discover, genotype and characterize typical and atypical CNVs from family and population genome sequencing. *Genome Res* (2011).
- 2 Willsey, A. J. *et al.* Coexpression networks implicate human midfetal deep cortical projection neurons in the pathogenesis of autism. *Cell* **155**, 997-1007 (2013).
- 3 Mariani, J. *et al.* Modeling human cortical development in vitro using induced pluripotent stem cells. *Proc Natl Acad Sci U S A* **109**, 12770-12775 (2012).
- 4 Kang, H. J. *et al.* Spatio-temporal transcriptome of the human brain. *Nature* **478**, 483-489 (2011).
- 5 Kim, J. E. *et al.* Investigating synapse formation and function using human pluripotent stem cell-derived neurons. *Proc Natl Acad Sci U S A* **108**, 3005-3010 (2011).
- 6 Okita, K. *et al.* A more efficient method to generate integration-free human iPS cells. *Nat Methods* **8**, 409-412 (2011).



## Supplementary Tables

### Supplementary Table 1. Participant characteristics.

Abbreviations: HC=head circumference; ADOS = Autism Diagnostic Observation Schedule; VBAS = Vineland Adaptive Behaviors Schedule; SS = Standard Score; COMM = Communication; DLS=Daily Living Skills; WGS= whole genome sequencing; RNASeq= high throughput RNA sequencing; NPC= neuronal progenitors (iPSC-derived); Rosette= rosette stage of neuronal differentiation; TD= day of terminal differentiation; ICC= immunocytochemistry.

*External Excel file*

**Supplementary Table 2.** Differentially expressed genes at day 11 (left) and day 31 (right).  
geneID: official gene symbol; log2FC: log2 Fold Change; FDR: FDR corrected p-value

*External Excel file*

**Supplementary Table 3.**

Day	GeneID	qPCR log2FC	RNAseq log2FC
11	<i>Brn2/POU3F2</i>	0.27	0.03
	<i>PAX6</i>	0.44	0.33
	<i>SOX1</i>	0.71	0.55
	<i>FOXP1</i>	1.31	1.35
	<i>DLX1</i>	1.74	2.93
	<i>DLX2</i>	3.02	3.09
	<i>Nkx2.1</i>	4.46	4.92
	<i>Gad67/GAD1</i>	1.14	0.87
	<i>Gad65/GAD2</i>	4.04	3.57
	<i>Vglut3/SLC17A8</i>	-2.49	-2.70
31	<i>Ctip2/BCL11B</i>	1.41	1.30
	<i>PAX6</i>	0.86	0.77
	<i>SOX1</i>	0.55	0.50
	<i>TBR1</i>	1.23	1.00
	<i>Brn2/POU3F2</i>	0.99	0.86
	<i>vGAT/SCL32A1</i>	3.53	3.50
	<i>Vglut1/SLC17A7</i>	0.51	0.37
	<i>Vglut2/SCL17A6</i>	1.02	0.84
		<b>corr coeff</b>	<b>0.98</b>

Validation of RNAseq calls by qPCR. 9 genes at differentiation day 11 and 8 genes at differentiation day 31. Day: day of differentiation; GeneID: gene symbol; qPCR log2FC: log2 fold change between probands and controls by qPCR; RNAseq log2FC: log2 fold change between probands and controls by RNAseq; corr coeff: correlation coefficient between logFC by qPCR and log2FC by RNAseq.

**Supplementary Table 4.** List of genes (as gene symbols) in each of the 24 modules inferred by WGCNA. Modules are listed in alphabetic order. Genes under the same column belong to the same module.

*External Excel file*

**Supplementary Table 5.** Overlap between DEGs and WGCNA modules.

**Table 5a.** Top: overlap between the DEGs up-regulated at day 11 and the WGCNA modules.  
Bottom: overlap between the DEGs down-regulated at day 11 and the WGCNA modules.

**Table 5b.** Top: overlap between the DEGs up-regulated at day 31 and the WGCNA modules.  
Bottom: overlap between the DEGs down-regulated at day 31 and the WGCNA modules.

*External Excel file*

**Supplementary Table 6.** Functional Enrichment analysis according to DAVID for the blue, brown, green, magenta, tan and yellow modules. Category: DAVID category; Term: DAVID category name; Count: number of DAVID genes in the list associated with particular annotation term; %: percentage of DAVID genes in the list associated with particular annotation term; PValue: nominal p-value; Genes: DAVID genes in the list (as gene symbols), also present in the particular annotation term; List Total: number of DAVID genes in the particular annotation term; Pop Hits: number of DAVID genes annotated in the particular annotation term on the background list ; PoP Total: number of DAVID genes on the background list mapped to any term in this ontology; Fold Enrichment; Bonferroni: Bonferroni corrected p-value; Benjamini: Benjamini corrected p-value; FDR: FDR corrected p-value.

*External Excel file*

**Supplementary Table 7.** Enrichment analysis results according to the Canonical Pathways database in MSigDB v4.0. # overlaps shown: number of significantly enriched gene sets listed; # genesets in collections: total number of gene sets present in the Canonical Pathway database in MSigDB v4.0; # genes in comparison (n): number of genes in the input list considered for analysis; # genes in universe (N): total number of genes in the Canonical Pathways database in MSigDB v4.0; Gene Set Name: gene set ID; # Genes in Gene Set (K): number of genes in the input list, also present in the particular gene set; Description: gene set description; Gene/Gene Set Overlap Matrix: connectivity matrix between gene sets and genes in the input list; Gene Symbol: gene symbol of the gene in the input list; Description: description of the particular gene in the input list.

**Supplementary Table 8.** List of top 100 most connected genes (hubs) in the green, yellow, blue, brown, magenta and tan modules. Also represented, for each module, the subsets of the top 100 hubs also differentially expressed at either TD11 or TD31. ALL: the full list of the top 100 hubs in the module; DGE11: subset of the top 100 hubs also differentially expressed at TD11; DGE31: subset of the top 100 hubs also differentially expressed at TD31.



**Supplementary Table 9**

List of primers used for qPCR

<b>Gene</b>	<b>Forward</b>	<b>Reverse</b>
GAPDH	AATCCCATCACCATCTTCCA	TGGACTCCACGACGTACTIONCA
POU3F2/ BRN2	AATAAGGCAAAAGGAAAGCAACT	CAAAACACATCATTACACCTGCT
PAX6	GTGTCTACCAACCAATTCCACAAC	CCCAACATGGAGCCAGATG
SOX1	GCAAGATGGCCCAGGAGAA	CCTCGGACATGACCTTCCA
FOXP1	AGAAGAACGGCAAGTACGAGA	TGTTGAGGGACAGATTGTGGC
BCL11B/ CTIP2	GAGTACTGCGGCAAGGTGTT	TAGTTGCACAGCTCGCACTT
TBR1	ATGGGCAGATGGTGGTTTTA	GACGGCGATGAACTGAGTCT
SCL32A1/ vGAT	AGGCTGGAACGTGACCAA	GGATGGCGTAGGGTAGGC
SLC17A7/ Vglut1	GAAACTCATGAACCCCCTCA	GGGAGATGAGCAGCAGGTAG
SCL17A6/ Vglut2	ATTCCATCAGCAGCCAGAGT	TTGCTCCATATCCCATGACA
ASCL1/ MASH1	GCTTCTCGACTTCACCAACTG	ATGCAGGTTGTGCGATCA
DLX1	TCCAGCCCCTACATCAGTTC	CCACCACCGTGCTCTTCT
DLX2	AGCAGCTATGACCTGGGCTA	AATTCAGGCTCAAGGTCCTC
GAD1/ GAD67	TCAAGTAAAGATGGTGTATGGGATA	GCCATGATGCTGTACATGTTG
GAD2/ GAD65	CTCATTGCCTTCACGTCTGA	GCTGTCTGTTCCAATCCCTAA
DLX6- AS1	TGATTCCTGTATGTATGGCAGCTA	GGTTTTCTTTGTCTCAGCAAT